AJNR Am J Neuroradiol 20:1491–1499, September 1999

Investigation of Apparent Diffusion Coefficient and Diffusion Tensor Anisotropy in Acute and Chronic Multiple Sclerosis Lesions

Andrew L. Tievsky, Thomas Ptak, and Jeffrey Farkas

BACKGROUND AND PURPOSE: **The various stages of multiple sclerosis (MS) are characterized by de- and remyelination as well as by inflammation. Diffusion MR imaging is sensitive to tissue water motion, which might correspond to these pathologic processes. Our purpose was to demonstrate differences in apparent diffusion coefficient (ADC) and diffusion tensor anisotropy in acute and chronic MS plaques and in normal-appearing brain.**

METHODS: **Twelve MS patients underwent conventional and full-tensor diffusion MR imaging with B = 1221 s/mm^2. Derivation of trace ADC and calculation of anisotropic scalars, including eccentricity, relative anisotropy (RA), and fractional anisotropy (FA) was performed on a per-pixel basis. Regions of interest of plaques and normal structures were determined on coregistered maps. MS lesions were classified as acute, subacute, or chronic on the basis of their appearance on conventional images and in relation to clinical findings.**

RESULTS: **Seven patients had acute plaques with a concentric arrangement of alternating high and low signal intensity on diffusion-weighted images. In nine acute lesions, plaque centers had high ADC with reduced anisotropy compared with rim, normal-appearing white matter (NAWM), and chronic lesions. The thin rim of diffusion-weighted hyperintensity surrounding the center showed variable ADC and anisotropic values, which were not statistically different from NAWM. Subacute and chronic MS lesions had intermediate ADC elevations/anisotropic reductions. Calculated FA pixel maps were superior to eccentricity or RA maps; however, quality was limited by signal-to-noise constraints.**

CONCLUSION: **ADC and diffusion anisotropic scalars reflect biophysical changes in the underlying pathology of the demyelinating process.**

The acute episode of multiple sclerosis (MS) is characterized by perivenular inflammation with axonal preservation and demyelination. A healing phase with incomplete remyelination follows. These events may occur in cyclic fashion, resulting in progressive deterioration of neuronal transmission and clinical function. Chronic lesions, after several such cycles, show hypocellularity of both glia and axons (1, 2).

When the mobility of a water molecule is dependent on direction, owing to factors of tissue micro- and macrostructure, such as in white matter, skeletal and cardiac muscle, renal medulla, and ocular lens, diffusion is said to be anisotropic (3). On diffusion-weighted MR images, normal white matter anisotropy is readily appreciated by analyzing the regions of hyperintensity produced on each unidirectional subset of the combined trace diffusion-weighted images. In contrast to isotropic diffusion acquisitions, which use only three orthogonal gradient pulses, data obtained from sampling of the complete diffusion tensor in at least six gradient directions are rotationally invariant with respect to the orientation of the applied gradients. The three principal diffusion axes may be determined by calculating the eigenvectors and their corresponding eigenvalues, $\lambda 1$, $\lambda 2$, and $\lambda 3$ as a prerequisite to the calculation of anisotropic scalars (4–6).

Received July 17, 1998; accepted after revision March 15, 1999.

Presented at the annual meeting of the American Society of Neuroradiology, Toronto, May 1997.

From the Department of Radiology, Georgetown University Medical Center, Washington, DC (A.L.T.); the Department of Radiology, Boston Medical Center (T.P.); and the Department of Radiology, Massachusetts General Hospital and Harvard Medical School, Boston (J.F.).

Address reprint requests to Andrew L. Tievsky, MD, Division of Neuroradiology CCC-2, Department of Radiology, Georgetown University Medical Center, 3800 Reservoir Rd NW, Washington, DC 20037.

© American Society of Neuroradiology

Anisotropic indexes derived from diffusion tensor eigenvalues represent reproducible values that reflect inherent biophysical properties of tissue structure. Whereas apparent diffusion coefficient (ADC) values for normal white and gray matter are virtually identical, cerebral white matter shows varying degrees of diffusion anisotropy, while the gray matter possesses nearly equal diffusion in all directions, or isotropy. Calculated scalar indexes show increasing values for subcortical U fibers, the internal capsule, the corona radiata, the forceps major and minor, and the corpus callosum, respectively. The inherent diffusion anisotropy of myelinated fiber tracts provides a parameter that might help characterize and possibly quantify the state of myelination of MS lesions using MR imaging.

ADC elevation in MS lesions has been reported previously (7–9). We proposed to quantify and compare ADC and diffusion tensor anisotropic scalars in regions of acute and chronic demyelination in MS as a correlate to the underlying pathology. A secondary goal of this project was to evaluate the quality and utility of calculated anisotropic maps calculated from full-tensor diffusion MR data.

Methods

Twelve patients with well-documented definite or clinically probable MS were examined with conventional and diffusion-weighted MR imaging. Studies were performed on a commercial 1.5-T scanner with echo-planar gradient strength of 10 mT/m. Full-tensor spin-echo (SE) diffusion-weighted imaging was performed in six gradient directions with B = 1221 s/mm^2. T2-weighted SE echo-planar images were obtained at each level with the diffusion gradients off for the purposes of ADC calculation (actual B = 57 s/mm^2). Technical factors were 6000/118/3 (TR/TE/excitations), 256 × 128 matrix, 40 × 20-cm field of view, 17 sections, and a total imaging time of approximately 2 minutes. Voxel dimensions were 1.56 mm in the *x* and *y* axes, with a 6-mm section thickness, for a voxel volume of 14.6 mm^3. Diffusion-weighted images and trace ADC maps were generated on-line. On a UNIX workstation, the eigenvalues λ1, λ2, and λ3 were computed from the diffusion tensor on a per-voxel basis and then used to generate anisotropic maps.

Calculated scalar indexes of tensor anisotropy, as described by Basser et al (5), included eccentricity, relative anisotropy (RA), and fractional anisotropy (FA).

Eccentricity (Ecc) of the diffusion tensor describes the ellipsoid nature of the principal and minor axes with reference to a circle:

$$\mathrm{Ecc} = \sqrt{1 - \lambda_3/\lambda_1}$$

Eccentricity is 0 for isotropic states and approaches 1 for the highly anisotropic condition of nearly unidirectional diffusion.

By separating the isotropic $(D)I$ and anisotropic components $(D)-(D)I$ of the diffusion deviatoric, other indexes may be calculated. The RA scalar represents a measurement of deviation from the isotropic state of the diffusion tensor:

$$\mathrm{RA} = \frac{\sqrt{D{:}D}}{\sqrt{(\mathrm{D})I{:}(\mathrm{D})I}}$$

where (D) is the effective diffusion tensor and $(D)I$ represents its isotropic component.

FA measures the fraction of the magnitude of the diffusion tensor that is anisotropic:

$$\mathrm{FA} = \sqrt{\frac{3}{2}}\sqrt{\frac{(\lambda_1 - \langle \mathrm{D}\rangle^2) + (\lambda_2 - \langle \mathrm{D}\rangle^2) + (\lambda_3 - \langle \mathrm{D}\rangle^2)}{\lambda_1{}^2 + \lambda_2{}^2 + \lambda_3{}^2}}$$

For RA and FA, values equal 0 for the isotropic condition, in which diffusion is equal in all directions and approach a value of 1 for extreme directional inequality, such as for the cylindrical cigar-shaped anisotropic medium, which closely models water diffusibility in myelinated fiber tracts.

Region of interest (ROI) determinations measuring 2 × 2 and 3 × 3 pixels were obtained manually on a Sun workstation. Regions whose measurements were contaminated by partial volume effects of CSF were excluded. ROIs of frontal subcortical normal-appearing white matter (NAWM) and deep gray matter in the posterior thalamus were used for reference values. A semiautomated program enabled simultaneous determination of diffusion-weighted imaging signal intensity, T2 echo-planar imaging signal intensity, ADC, three eigenvalues, eccentricity, FA, and RA on coregistered image maps. Statistical analysis was performed by calculating correlation coefficients and by applying independent and correlated two-tailed *t*-tests where appropriate.

MS lesions were classified by consensus of two neuroradiologists as being acute, subacute, or chronic on the basis of T1 and T2 relaxation characteristics, the presence of contrast enhancement after administration of a gadolinium chelate, and surrounding edema (10). Plaques that were considered to be acute were characterized by peripheral contrast enhancement after administration of gadopentetate, by central T1 hypointensity/T2 hyperintensity, and, in most cases, by a rim of T2 edema. These lesions frequently corresponded to neurologic deficits. Using commonly accepted criteria, other plaques were categorized as either subacute, owing to the presence of edema or contrast enhancement, or chronic, on the basis of morphology and signal characteristics. Anisotropic maps were evaluated for image quality by consensus of two neuroradiologists.

Results

Clinical and radiologic findings are summarized in Table 1. A complete data set consisting of ADC and anisotropic scalars was determined for 46 MS plaques in 12 patients. Global results of plaque classification and measurements are given in Table 2. Analysis of all plaques revealed an inverse relationship between ADC and anisotropic indexes. FA, RA, and eccentricity values were closely correlated, in accordance with previous studies of these parameters (3, 5) (Table 3).

FA maps were judged superior to RA and eccentricity for general image quality in all cases. All calculated maps, however, were degraded by random noise imposed by relative signal-to-noise (S/N) constraints, which have been reported previously (11). Accordingly, for 18 lesions, additional ADC and FA measurements were obtained by hand ROI measurements.

In seven of 12 patients, a total of nine acute demyelinating plaques were identified. These plaques were characterized by a concentric arrangement of

TABLE 1: Summary of clinical and imaging findings in 12 patients with multiple sclerosis

Patient	Age/Sex	Disease Duration	Duration of Present Symtpoms or Exacerbation	Clinical Findings	Plaque Morphology and Distribution	Contrast Enhancement
B.A.	23/M	5 y	1.5 wk	Right-handed numbness	Few: polyphasic, acute/subacute, periventricular, acute center/rim	+
B.E.	29/F	1.2 y	1.2 y	Left paresthesias, generalized lower extremity weakness (rapidly progressive course)	Multiple: polyphasic, subacute/chronic, periventricular and large pontine	+
B.O.	53/F	30 y	No acute change	Chronic progressive dementia	Multiple: monophasic, chronic, periventricular	−
F.E.	65/F	>20 y	No acute change	Bilateral lower extremity weakness and numbness	Multiple: monophasic, chronic, periventricular	−
H.U.	22/F	Initial presentation probable MS	2–4 wk	Right facial numbness, ataxia, diplopia	Multiple: polyphasic, acute/subacute center/rim pattern	+
J.E.	30/M	>5 y	No acute change	Generalized weakness	Multiple: monophasic, chronic, periventricular and subcortical plaque	−
K.O.	33/F	Initial presentation probable MS	2–4 wk	Optic neuritis	Multiple: polyphasic, periventricular, center/rim pattern	+
L.A.	33/F	12 y	4+ wk	Diploplia, dizziness, internuclear ophthalmoplegia	Multiple: monophasic, small, chronic, periventricular	−
N.O.	15/F	10 mo (Schilder's) probable MS	6 wk	Right-sided weakness and numbness	Single large plaque in corpus callosum, center/rim pattern	+
P.U.	26/M	10 mo	0–8 wk	Left-sided face and hand numbness, bilateral lower extremity weakness, fecal incontinence, urinary retention	Multiple: polyphasic, acute/subacute, periventricular, center/rim pattern	+
V.Y.	24/M	7 mo	2 wk	Quadriparesis, weakness in extremities L > R, lower > upper	Multiple: polyphasic, acute/subacute, periventricular, center/rim pattern	+
Y.O.	43/F	9 mo	1–2 wk	Vertigo, left sensory disturbance, diplopia on right gaze	Multiple: polyphasic, acute/subacute, periventricular, center/rim pattern	+

TABLE 2: Mean ADC mm²/s, T2 signal intensity, and anisotropic indexes for acute ring plaques, subacute enhancing lesions, and chronic plaques in 12 patients with MS

	Thalamus	NAWM	Acute Plaque Center	Acute Plaque Rim	Subacute Enhancing Plaques	Chronic Plaques
ADC						
Mean	.00070	.00079	.00159	.00092	.00099	.00108
SD	.00009	.00011	.00062	.00029	.00050	.00022
T2						
Mean	180.4	128.2	351.2	235.3	213.9	280.8
SD	54.4	23.8	218.6	118.6	116.2	76.9
FA						
Mean	.338	.404	.189	.341	.278	.289
SD	.113	.110	.096	.165	.149	.079
RA						
Mean	.315	.398	.232	.342	.277	.291
SD	.122	.108	.187	.264	.147	.059
ECC						
Mean	.714	.753	.543	.651	.608	.679
SD	.100	.073	.118	.088	.242	.060

Note.—ADC indicates apparent diffusion coefficient; FA, fractional anisotropy; RA, relative anisotropy, ECC, eccentricity; NAWM, normal-appearing white matter.

TABLE 3: Correlation matrix for anisotropy indexes and ADC for 46 MS lesions in 12 patients

	ADC	ECC	FA	RA
ADC	1			
ECC	−0.7573*	1		
FA	−0.7091*	0.9545*	1	
RA	−0.6839*	0.9443*	0.987*	1

Note.—ADC indicates apparent diffusion coefficient; ECC, eccentricity; FA, fractional anisotrophy; RA, relative anisotrophy.

* $P < .01$.

alternating high and low signal intensity on diffusion-weighted images, rim enhancement after administration of contrast material, and peripheral edema (Figs 1–3). These lesions showed a hypointense center on diffusion-weighted images, characterized by high ADC values and T2 prolongation, surrounded by a hyperintense rim, with variable ADC and intermediate T2 signal hyperintensity. Typically, there was peripheral edema, distinguished by moderate increases in ADC and T2 signal. The diffusion-weighted imaging appearance of the center and rim can be explained by central dephasing due to high ADC, with T2 ''shine through'' in the rim caused by relatively unaffected ADC values, comparable to NAWM, in association with elevated T2 signal. Chronic plaques had higher ADC values and a tendency toward isotropy, as compared with NAWM, and were of intermediate signal intensity relative to the centers of acute lesions. A typical chronic case of MS is illustrated in Figure 4.

The ADC and FA median and range for categorized plaques and normal structures are summarized graphically in Figure 5. Correlated and independent two-tailed *t*-tests showed that statistically significant relationships of ADC and FA were complementary: ADC acute plaque center > ADC acute plaque rim ($P < .01$); FA acute plaque center < FA acute plaque rim ($P < .01$); ADC acute plaque center > ADC NAWM ($P < .05$) and thalamus ($P < .05$); and FA acute plaque center < NAWM ($P < .05$) and thalamus ($P < .05$). There was considerable variability and lack of statistical significance between ADC and FA measurements of acute plaque rims and NAWM or thalamus.

Differences between ADC and FA measurements of 64 subacute and chronic plaques lacked statistical significance. Accordingly, these lesions were grouped together. ADC subacute/chronic plaques > ADC NAWM ($P < .01$) and thalamus ($P < .001$); FA subacute/chronic plaques < FA NAWM ($P < .05$); ADC subacute/chronic plaques < ADC acute plaque center ($P < .05$); FA subacute/chronic plaques > FA acute plaque center ($P < .01$).

Discussion

Previous investigators have also described ADC elevation in MS lesions (7). Christianson et al (9) reported ADC values to be greater in acute than in chronic MS lesions, which were both higher than NAWM. This is in agreement with prior nonisotropic studies. In addition, ADC was elevated in the NAWM of MS patients as compared with control subjects (8, 9).

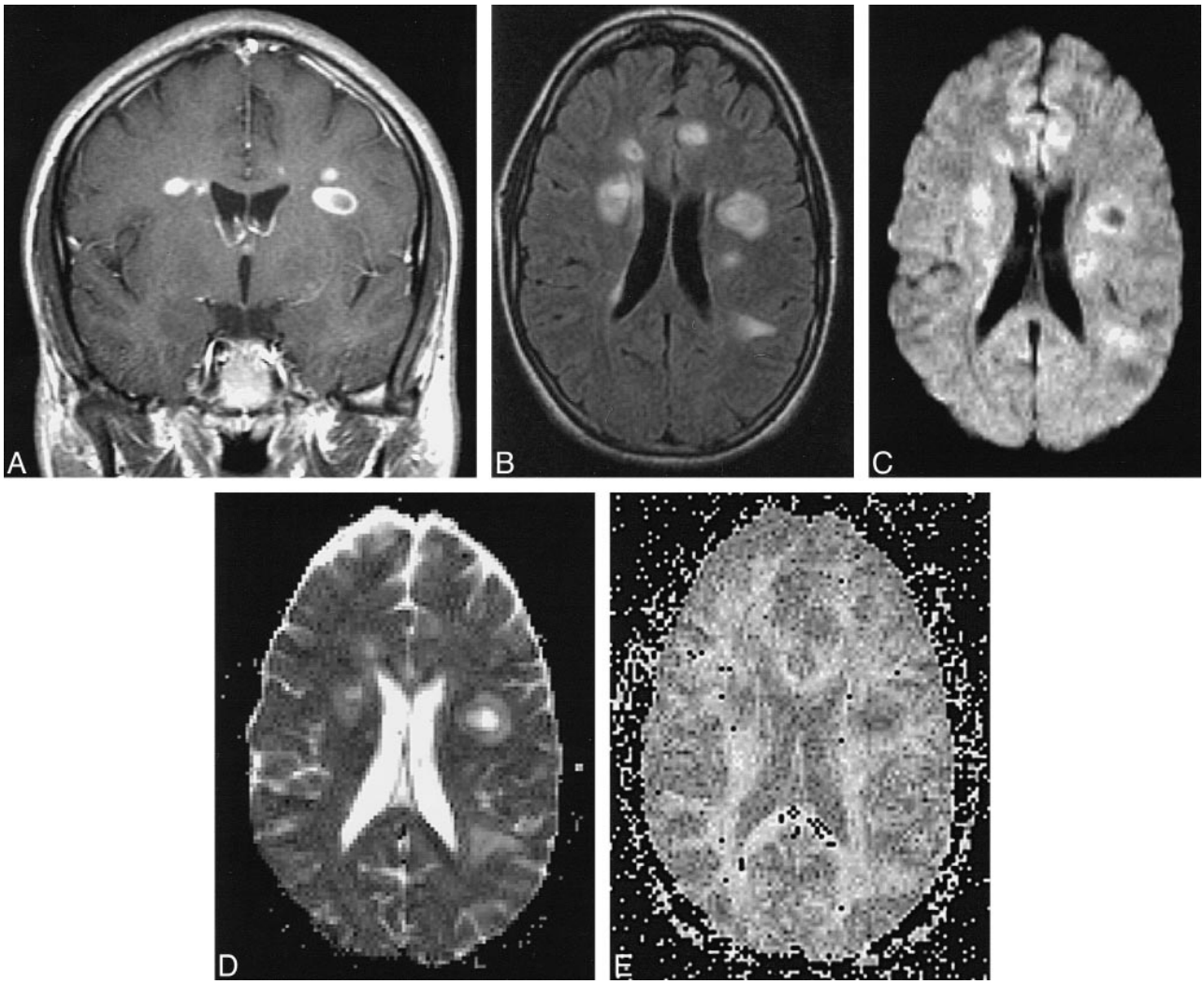

FIG 1. Patient H.U.: 22-year-old woman with acute plaques and multiple neurologic signs and symptoms of 2 to 4 weeks' chronicity at first presentation of MS.

A–F, Multiple monophasic ring lesions are identified on T1-weighted contrast-enhanced (*A*) and FLAIR (*B*) images. Lesion centers show hypointensity on diffusion-weighted image (*C*) with corresponding increased diffusibility (brightness) on calculated ADC map (*D*), caused by increased water mobility in regions of acute inflammation. Reduction in anisotropy in these regions is present on calculated maps of eccentricity (*E*) and FA (*F*). Note that region of peripheral edema is readily differentiated from thin plaque rim on ADC map. ADC values: NAWM, 0.00081; left periventricular acute plaque center, 0.00211; left periventricular acute plaque rim, 0.00124. FA values: NAWM, 0.299; left periventricular acute plaque center, 0.111; left periventricular acute plaque rim, 0.162.

The concentric ring appearance of acute lesions we observed on diffusion-weighted images is in accordance with serial studies of plaque evolution on MR images in patients with relapsing-remitting MS (10). Increased diffusivity with anisotropic reduction in the plaque center may be secondary to the combined effects of increased extracellular water and loss of myelin. Blood-brain barrier disruption in acute MS, due to astrocytic damage or functional impairment of intact endothelium or both, results in an increase in extracellular water in the perivenular region, which constitutes part of the plaque center. Oligodendrocyte damage also occurs early in plaque development, resulting in demyelination and alteration of axonal conduction, which is a significant contributor to neurologic dysfunction. Electron microscopy studies have shown the presence of inflammatory infiltrates of lymphocytes and lipid-engulfing macrophages, swollen oligodendroglia, as well as expansion of extracellular volumes. In an acute plaque, these pathologic processes evolve in a centrifugal manner. The rim of an acute lesion is characterized by histopathologic findings of capillary alterations, which are thought to account for ring enhancement of these lesions. We speculate that the variability of ADC and anisotropic scalars in the plaque rim in the region of active demyelination, as defined in this study, represents the presence of vasogenic edema in the extracellular space superimposed on cytotoxic edema of oligodendroglia.

Chronic MS lesions are characterized pathologically by zones of myelin loss with axonal preser-

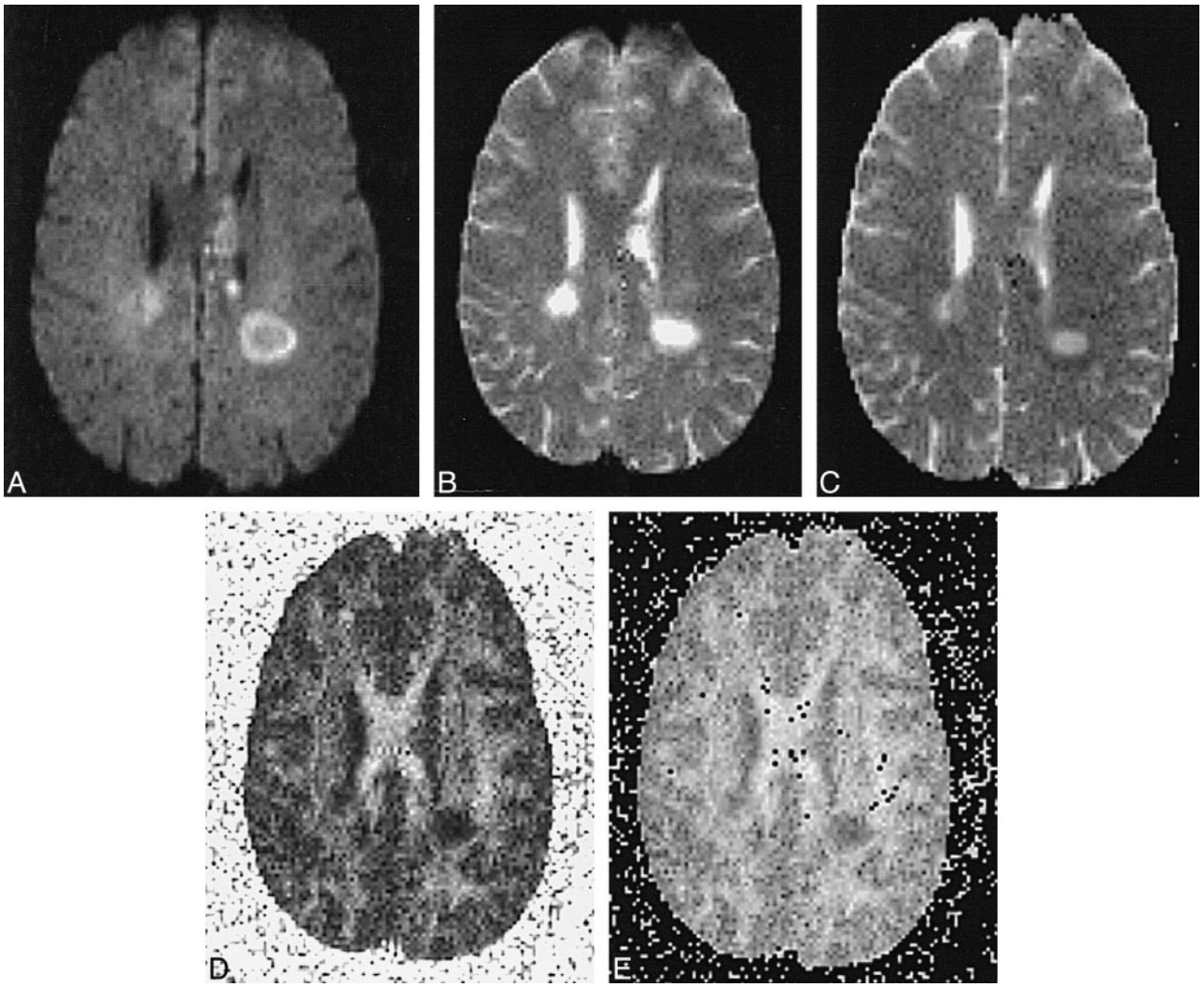

FIG 2. Patient V.Y: 24-year-old man with 7-month history of relapsing-remitting MS presented with quadriparesis, most severe in upper extremities, and left periventricular acute plaque.

A–E, Note delineation of the hyperintense rim on diffusion-weighted image and relative hypointensity of lesion center (*A*). T2-weighted echo-planar image shows marked central hyperintensity and slightly lower signal in rim (*B*). Center has increased diffusibility, appearing almost as bright as CSF, and has a low ADC value (dark) in the rim on calculated ADC map (*C*). FA (*D*) and eccentricity (*E*) maps reveal intermediate anisotropic values in rims relative to lesion centers, which approach isotropy. ADC values: NAWM, 0.00071; left periventricular acute plaque center, 0.00136; left periventricular acute plaque rim, 0.00066. FA values: NAWM, 0.430; left periventricular acute plaque center, 0.135; left periventricular acute plaque rim, 0.362.

vation, reactive astrogliosis, and absence of acute inflammation. Extracellular water is increased relative to uninvolved white matter. These histopathologic findings would seem to correlate well with intermediate ADC elevations and a tendency toward isotropy.

Considerable variability in ADC and anisotropic scalars was observed between measurements of morphologically similar lesions in the present study. In addition to intrinsic differences in diffusivity, measurements of MS plaques were affected by the technical limitations of echo-planar diffusion-weighted MR imaging. Relatively low S/N ratios, echo-planar artifacts, and other factors affecting the magnitude and uniformity of image signal intensity, while not objectionable for qualitative diagnostic purposes, produce significant obstacles to quantitative data analysis. Previous experience has shown that ADC and anisotropic values may vary 15% or more among individuals or in the same individual on different scanning examinations, including those that are performed on the same day. Accordingly, we have found it difficult to compare diffusion parameters in normal and abnormal brain structures in small groups of subjects. Previous attempts to introduce healthy control subjects have confounded data analysis (12, 13). Rather, this MS population was studied on a per-patient basis using apparently uninvolved brain structures as internal controls. Nevertheless, consistent patterns of anisotropic reduction and ADC elevation in plaques in various stages of evolution emerged in this study. It is anticipated that future improvements in scanner hardware in co-

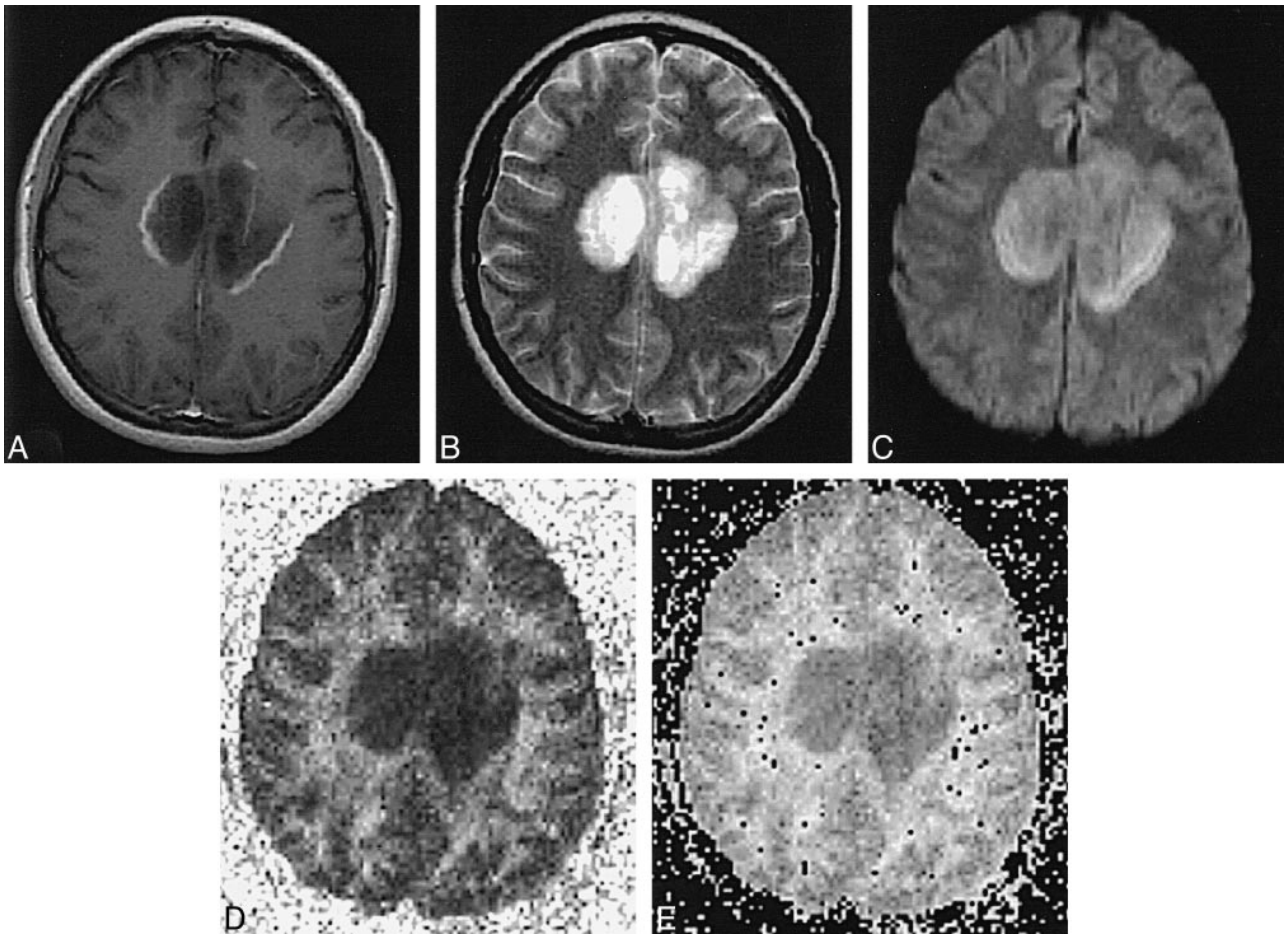

FIG 3. Patient N.O.: 15-year-old girl with 10-month history of Schilder's MS variant.

A–E, Unusual bihemispheric callosal plaque shows a mixed pattern with rim enhancement on T1-weighted contrast-enhanced (*A*) and T2-weighted (*B*) images. Diffusion-weighted image shows moderate hyperintensity, caused by T2 shine through in lesion center, with hyperintense rim (*C*). Calculated ADC map (not shown) revealed increased diffusibility in lesion center with slight decrease in rim. Calculated maps of FA (*D*) and eccentricity (*E*) show marked tendency toward isotropy in lesion center, with minimal anisotropic reduction in rim. ADC values: NAWM, 0.00068; acute plaque center, 0.00155; acute plaque rim, 0.00072. FA values: NAWM, 0.568; acute plaque center, 0.176; acute plaque rim, 0.312.

ordination with the development of clinically practical non–echo-planar diffusion pulse sequences will improve the reliability of absolute diffusion measurements.

Another limitation of the methodology in this study is the failure to account for the inherent spatial/anatomic dependence of anisotropic measurements, which may result in erroneous comparisons of voxels in different white matter regions (5, 14). For example, these anatomic factors produce anisotropic differences between acute plaque rim and NAWM, in addition to histopathologic factors. In general, owing to differences in local fiber organization, the true significance of absolute anisotropic measurements can only be appreciated in relation to normal contralateral brain structures. However, since most MS patients harbor microscopic or macroscopic disease in contralateral periventricular white matter, corona radiata, and subcortical white matter, use of ''mirror'' measurements or other internal controls for comparing ROIs may not be accurate.

Also, our classification of plaques in the subacute category may not be entirely accurate in view of the absence of serial MR examinations in these patients. While the true age range of the lesions is unknown, their morphologic characteristics suggest that they were undergoing remyelination (10).

The natural history of MS includes the gradual accumulation and increase in size of demyelinating plaques. While most of this activity is clinically silent, the total lesion burden over a number of years may result in significant clinical disability. Observations of increased T2 relaxation times and abnormal magnetization transfer ratios in NAWM in MS patients are thought to represent the presence of diffuse microscopic disease that is frequently found on pathologic examinations of these patients (15). However, volume measurements of regions of T2 hyperintensity on conventional MR images do not correlate well with indexes of clinical disability (16–18). Furthermore, studies of postmortem specimens have shown that

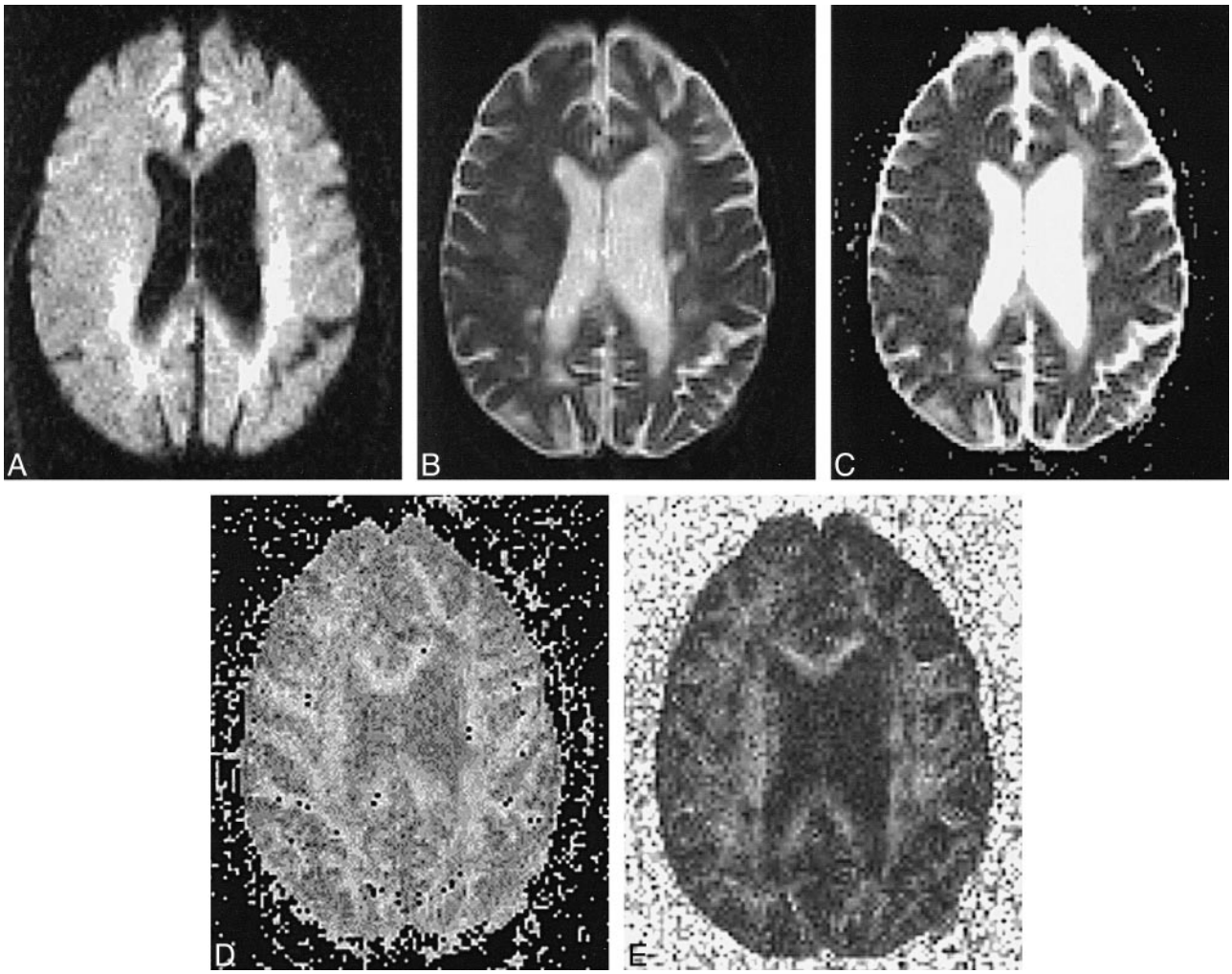

FIG 4. Patient B.O.: 53-year-old woman with 40-year history of MS, presenting with dementia. T2 hyperintensity and ADC elevation are apparent with loss of white matter anisotropy in multiple chronic periventricular and subcortical plaques.

A–E, Diffusion-weighted image (*A*), T2-weighted echo-planar image (*B*), ADC map (*C*), and calculated maps of eccentricity (*D*) and FA (*E*). ADC values: NAWM, 0.00097; right corona radiata chronic plaque, 0.00083; left periventricular chronic plaque, 0.00071. FA values: NAWM, 0.334; right corona radiata chronic plaque, 0.289; left periventricular chronic plaque, 0.445.

there is considerable pathologic heterogeneity in chronic MS lesions with respect to the amount of extracellular water and axonal loss, and do not correspond well to MR appearance on T1- or T2-weighted images (19, 20).

With future anticipated improvements in statistical reliability, it is likely that anisotropic measurements of NAWM might provide an index of fiber myelination that reflects the cumulative lesion burden not currently obvious on routine images. Hence, one might speculate that a proposed future application for tensor MR imaging would be in the serial evaluation of lesion load in patients with long-standing disease, such as in comparison with histograms of serial whole-brain diffusion anisotropic studies that have been thresholded to remove CSF effects. Longitudinal epidemiologic studies will be necessary to confirm this hypothesis.

Conclusion

Alterations in ADC and diffusion tensor anisotropy accompany the changing histopathology of demyelinating processes. Typical acute plaques show a concentric ring pattern on diffusion-weighted images. The center of an acute plaque is characterized by marked T2 hyperintensity, high ADC, and marked reduction of anisotropy as compared with the rim, NAWM, and chronic plaques. Histologically, the center region is composed of inflammatory cellular exudates with demyelinated axons. The surrounding rim shows mixed ADC and anisotropic values as compared with normal structures, moderate T2 signal hyperintensity, and enhancement after administration of a gadolinium chelate. The plaque rim is thought to represent the area of acute demyelination. Chronic plaques, which have been shown pathologically to be regions of reduced cellularity with a relative in-

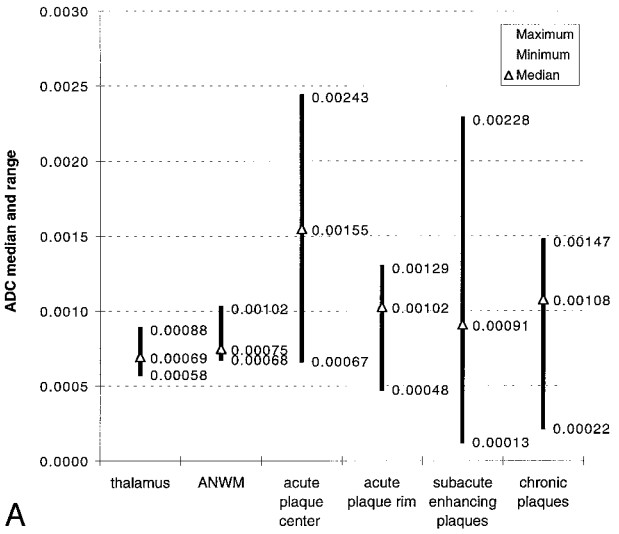

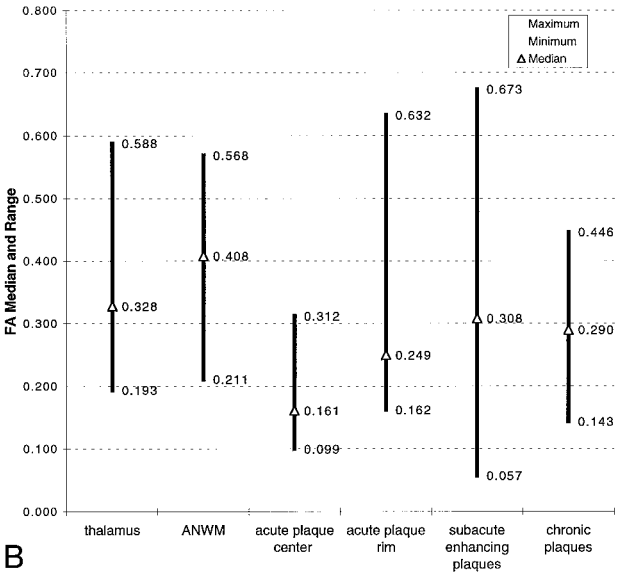

FIG 5. *A,* ADC median and range of MS plaques as compared with deep gray matter (thalamus) and NAWM.

B, FA median and range of MS plaques as compared with deep gray matter (thalamus) and NAWM.

crease in extracellular water, exhibit intermediate ADC elevation and moderate reductions in anisotropic values as compared with NAWM.

References

1. Ludwin SK. **Central nervous system remyelination: studies in chronically damaged tissue.** *Ann Neurol* 1994;36(Suppl):143–145
2. Weinshenker BG. **Natural history of multiple sclerosis.** *Ann Neurol* 1994;36(Suppl):6–11
3. Basser PJ, Mattiello J, Le Bihan D. **Anisotropic diffusion: MR diffusion tensor imaging.** In: Le Bihan D, ed. *Diffusion and Perfusion Magnetic Resonance Imaging: Applications to Functional MRI.* New York: Raven; 1995:140–149
4. Douek P, Turner R, Pekar J, Patronas N, Le Bihan D. **MR color mapping of myelin fiber orientation.** *J Comput Assist Tomogr* 1991;15:923–929
5. Basser PJ, Pierpaoli C. **Microstructural and physiological features of tissues elucidated by quantitative-diffusion-tensor MRI.** *J Magn Reson B* 1996;111:209–219
6. Hsu EW, Mori S. **Analytical expressions for the NMR apparent diffusion coefficient in an anisotropic system and a simplified method for determining fiber orientation.** *Magn Reson Med* 1995;34:194–200
7. Larsson HB, Thomsen C, Frederiksen J, Stubgaard AM, Henriksen O. **In vivo magnetic resonance diffusion measurement in the brain of patients with multiple sclerosis.** *Magn Reson Imaging* 1992;10:7–12
8. Horsfield MA, Lai M, Webb SL, et al. **Apparent diffusion coefficients in benign and secondary progressive multiple sclerosis by nuclear magnetic resonance.** *Magn Reson Imaging* 1996;36:393–400
9. Christiansen P, Gideon P, Thomsen D, Stubgaard M, Henriksen O, Larsson HBW. **Increased water self-diffusion in chronic plaques and in apparently normal white matter in patients with multiple sclerosis.** *Acta Neurol Scand* 1992;87:195–199
10. Guttman CRG, Sungkee SA, Liangge H, Kikinis R, Jolesz FA. **The evolution of multiple sclerosis lesions on serial MR.** *AJNR Am J Neuroradiol* 1995;16:1481–1491
11. Wu O, Weiskoff RM, Copen WA, Rosen BR, Sorensen AG. **Comparison of scalar metrics of anisotropy in ischemic human brain using diffusion weighted magnetic resonance imaging.** In: *Proceedings of the International Society of Magnetic Resonance in Medicine; April 12–18, 1997; Vancouver, BC, Canada*
12. Tievsky AL, Gonzalez RG, Rosen BR, Sorensen AG. **Investigation of ADC changes in acute cerebral infarction with ischemia.** Presented at the annual meeting of the American Society of Neuroradiology, Philadelphia, May 1998
13. Tievsky AL, Schaefer PW, Gonzalez RG, Rosen BR, Sorensen AG. **Full tensor diffusion-weighted imaging of white matter shear injury.** Presented at the annual meeting of the American Society of Neuroradiology, Toronto, May 1997
14. Moseley ME, Kucsharczyk J, Asgari HS, Norman D. **Anisotropy in diffusion-weighted MRI.** *Magn Reson Med* 1991;19: 321–326
15. Barbosa S, Blumhardt LD, Roberts N, Lock T, Edwards RH. **Magnetic resonance relaxation time mapping in multiple sclerosis: normal appearing white matter and the "invisible" lesion load.** *Magn Reson Imaging* 1994;12:33–42
16. Gass A, Barker GJ, Kidd D. **Correlation of magnetization transfer ratio with clinical disability in multiple sclerosis.** *Ann Neurol* 1994;36:62–67
17. Simon JH. **Contrast-enhanced MR imaging in the evaluation of treatment response and prediction of outcome in multiple sclerosis.** *J Magn Reson Imaging* 1997;7:29–37
18. Mammi S, Filippi M, Martinelli V, et al. **Correlation between brain MRI lesion volume and disability in patients with multiple sclerosis.** *Acta Neurol Scand* 1996;94:93–96
19. Barnes D, Munro PMG, Youl BD, Prineas JW, McDonald WI. **The long-standing MS lesion.** *Brain* 1991;114:1271–1280
20. Jacobs L, Kinkel WR, Ploachini I, Kinkel RP. **Correlations of nuclear magnetic imaging, computerized tomography, and clinical profiles in multiple sclerosis.** *Neurology* 1986;36:27–34